Supporting Information

Expediting hole transfer via surface states in hematite-based composite photoanodes

Lili Gao[a], Peng Wang[a], Huan Chai[a], Shuwen Li[a], Jun Jin[a] and Jiantai Ma[a, b*]*

a State Key Laboratory of Applied Organic Chemistry (SKLAOC), The Key Laboratory of Catalytic Engineering of Gansu Province, Key Laboratory of Advanced Catalysis of Gansu Province, College of Chemistry and Chemical Engineering, Lanzhou University, Lanzhou 730000, P. R. China

b School of Chemical Engineering and Technology, Tianshui Normal University, Tianshui, Gansu, 741001, P. R. China

Corresponding Author* E-mail: majiantai@lzu.edu.cn; jinjun@lzu.edu.cn.

Characterization

Field emission scanning electron microscopy (SEM, type of Hitachi S-4800), transmission electron microscopy (TEM) and high-resolution TEM (HRTEM) (type of Tecnai F30) were used to characterize the morphology and structure of all photoanodes. The energy-dispersive X-ray spectroscopy (EDS) elemental mapping was to investigate via an annular darkfield detector under TEM. X-ray diffraction spectra (XRD) were applied to analyze the crystallinity of the catalysts, which were conducted on a Rigaku D/max-2400 diffractometer with Cu Kα radiation. X-ray photoelectron spectroscopic (XPS) were used to study the elecment composition and valence state by a Kratos Axis Nova X-ray photoelectron spectrometer with monochromated Al Kα as the X-ray source that was manipulated at 15 kV and 10 mA and C 1s was set as the energy reference (284.8 eV). The light absorption capacity of all photoelectrodes were determined by UV/Vis absorption spectra (Hitachi U-4000) with $BaSO_4$ as the reference.

Photoelectrochemical measurements

All the photoelectrochemical measurements were conducted on an electrochemical workstation (CHI760E, CH Instruments Co.). A three-electrode system was applied, composed of electrolyte (1 M KOH aqueous solution), a working electrode (the as-prepared photoanode), a counter electrode (Pt electrode) and a reference electrode (Ag/AgCl electrode immersed in a satuated KCl solution). The contacted area of electrode with the electrolyte was fixed to 1 square centimeter. The light source was a 300 W Xenon arc lamp (Perfect Light solar simulator) with an AM 1.5G filter, and the

light intensity irradiated on the photanode was adjusted by changing the distance until it was 100 mW cm^{-2} (1 sun illumination) exactly. All the mentioned potential was versus the reversible hydrogen electrode (RHE). Linear sweep voltammetry (LSV) curves were performed at the scanning rate of 10 mV s^{-1}, and the potential range was set as 0.5-1.6 V. Cyclic voltammetry (CV) curves were carried out to observe surface states, and the CV curves in dark were conducted from 1.7-0.4 V in negative polarity, whereas those under illumination were conducted from 0.4-1.6 V in positive polarity. The scan rate of the above CV curve was 0.2 V s^{-1}. Photoelectrochemical electrochemical impedance spectroscopy (PEIS) were carried out as follows: the bias potential from 0.5 to 1.3 V_{RHE} with an interval of 0.05 V, the ac voltage amplitude of 5 mV, the frequency range from 1 to $\sim 10^5$ Hz. Mott-Schottky (M-S) spectra were obtained under dark condition, and the applied potential range is 0.3-1.4 V_{RHE}, the scan rate is 20 mV s^{-1} and the frequency is 1 kHz.

Equations related in this work

1. Calculation of Applied bias photon to current conversion efficiency (ABPE)[1]

$$ABPE(\%) = \frac{J \times (1.23 - V_b)}{P_{total}} \times 100\% \qquad \text{equation 1}$$

where J is the measured photocurrent density (mA cm^{-2}), V_b is the applied potential (V_{RHE}) and P_{total} is the light intensity of AM 1.5G (100 mW cm^{-2}).

2. Mott-Schottky (M-S) analysis[2]

$$N_d = \frac{2}{e\varepsilon\varepsilon_0} \times \left(\frac{d\left(\frac{1}{C^2}\right)}{dV_s} \right)^{-1} \qquad \text{equation 2}$$

where e is the charge quantity of an electron (1.6×10^{-19} C), vacuum permittivity (ε_0) is 8.85×10^{-12} F m^{-1}, and relative permittivity (ε) is 80 for α-Fe_2O_3[3]. C (F cm^{-2}) is the space charge capacitance in the semiconductor (obtained from M-S curves), and Vs (V) is the applied potential for M-S curves.

3. Theoretical maximum photocurrent density (J_{abs})[2]

Theoretical maximum photocurrent density (J_{abs}) is the photocurrent density assuming that all absorbed photons can be converted into current (i.e., APCE = IPCE/LHE = 100%), it is a constant with the AM 1.5G spectrum and the light harvesting efficiency of the fixed photoelectrode. In the case of J_{abs}, it can be calculated according to the following equation:

$$J_{abs} = \int_{\lambda 1}^{\lambda 2} \frac{\lambda \times LHE(\lambda) \times P(\lambda)}{1240} d(\lambda) \qquad \text{equation 3}$$

where λ and $P(\lambda)$ are the light wavelength (nm) and the corresponding power density (mW cm^{-2} nm^{-1}) for the standard solar spectrum AM 1.5G (ASTMG-173-03), respectively, $LHE(\lambda)$ is light absorption efficiency.

4. The surface charge injection efficiency ($\eta_{surface}$) and bulk charge separation efficiency (η_{bulk})[2]

Charge separation efficiency (η_{sep} or η_{bulk}, the yield of photogenerated holes that have reached the semiconductor/electrolyte interfaces) and surface charge transfer efficiency (η_{trans} or $\eta_{surface}$, the yield of holes that are involved in water oxidation reaction after reaching the electrode/electrolyte interfaces) of the as-obtained photoanodes can be calculated using the following equations:

$$\eta_{bulk} = \frac{J_{Na_2SO_3}}{J_{abs}}$$ equation 4

$$\eta_{surface} = \frac{J_{H_2O}}{J_{Na_2SO_3}}$$ equation 5

$J_{Na_2SO_3}$ and J_{H_2O} are the photocurrent densities measured in 1 M KOH with and without 1 M Na_2SO_3, respectively.

Supplemental Figures

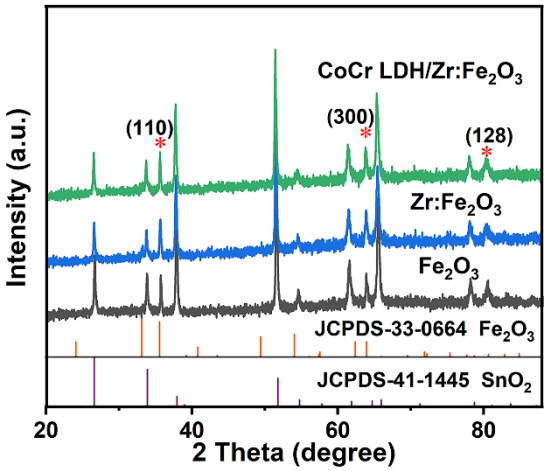

Figure S1. XRD patterns of the as-prepared photoanodes.

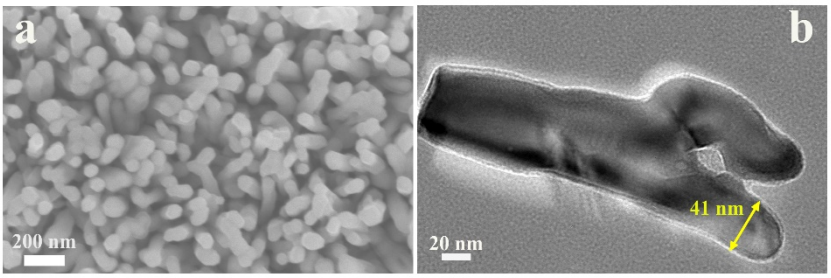

Figure S2. SEM and TEM images of Zr:Fe_2O_3 sample.

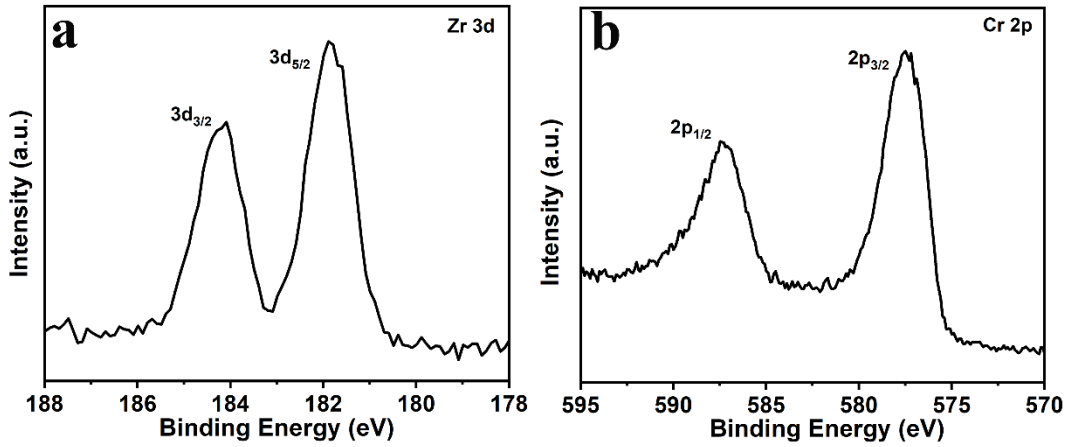

Figure S3. XPS spectra of (a) Zr 3d and (b) Cr 2p for the as-prepared photoanodes.

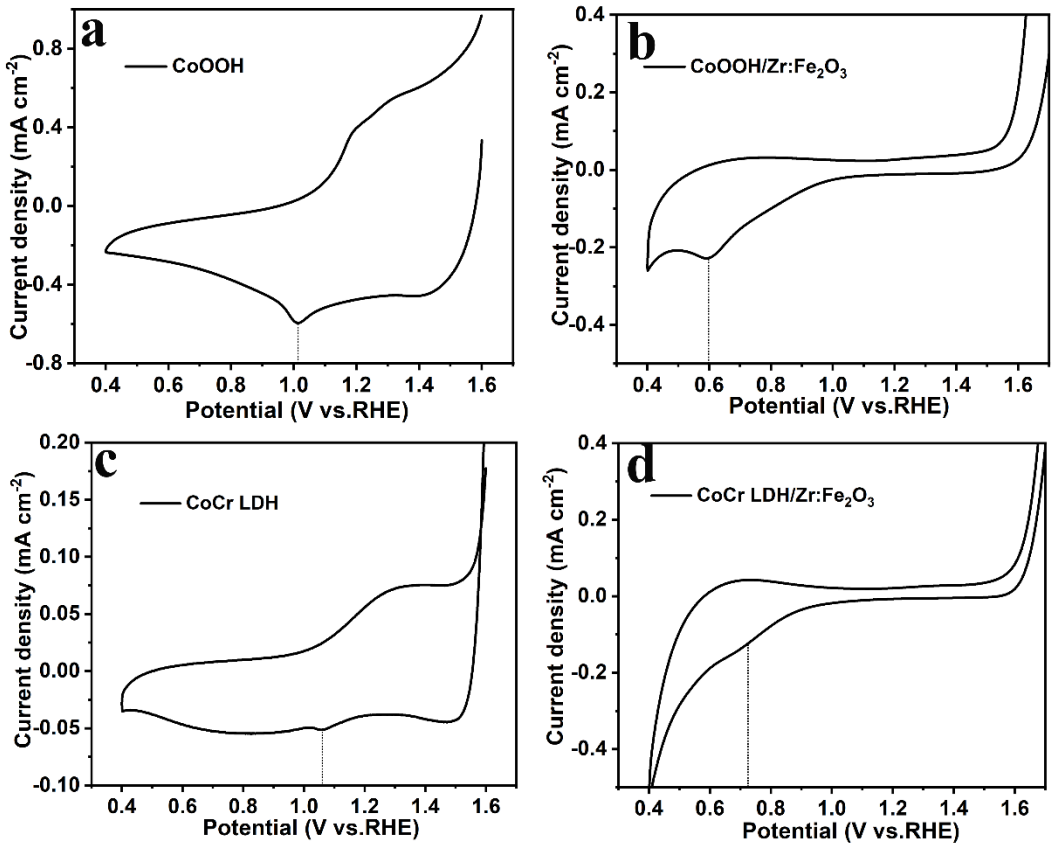

Figure S4. CV curves in dark at the scan rate of 200 mV s^{-1} of (a) CoOOH, (b) CoOOH /Zr:Fe_2O_3, (c) CoCr LDH, and (d) CoCr LDH/Zr:Fe_2O_3 recorded immediately after holding the potential at 1.85 V_{RHE} for 1 min.

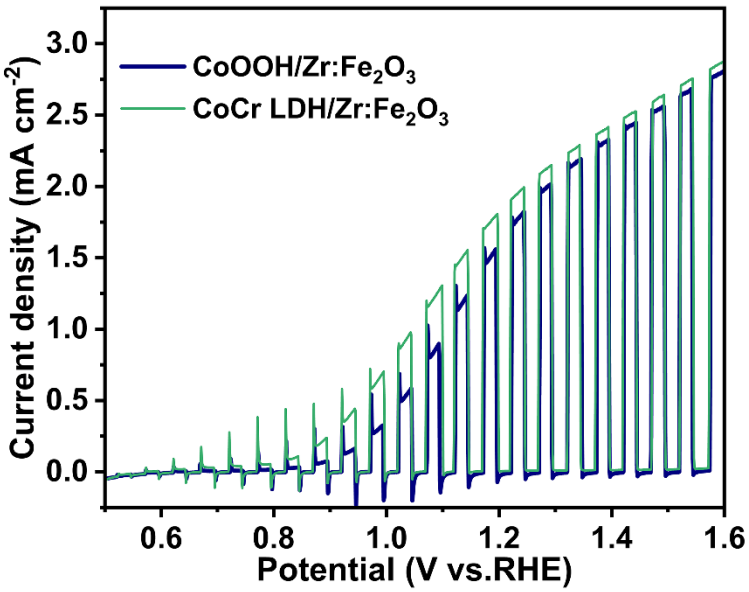

Figure S5. (a) Chopped LSV curves measured in 1 M KOH of CoOOH /Zr:Fe_2O_3 and CoCr LDH/Zr:Fe_2O_3.

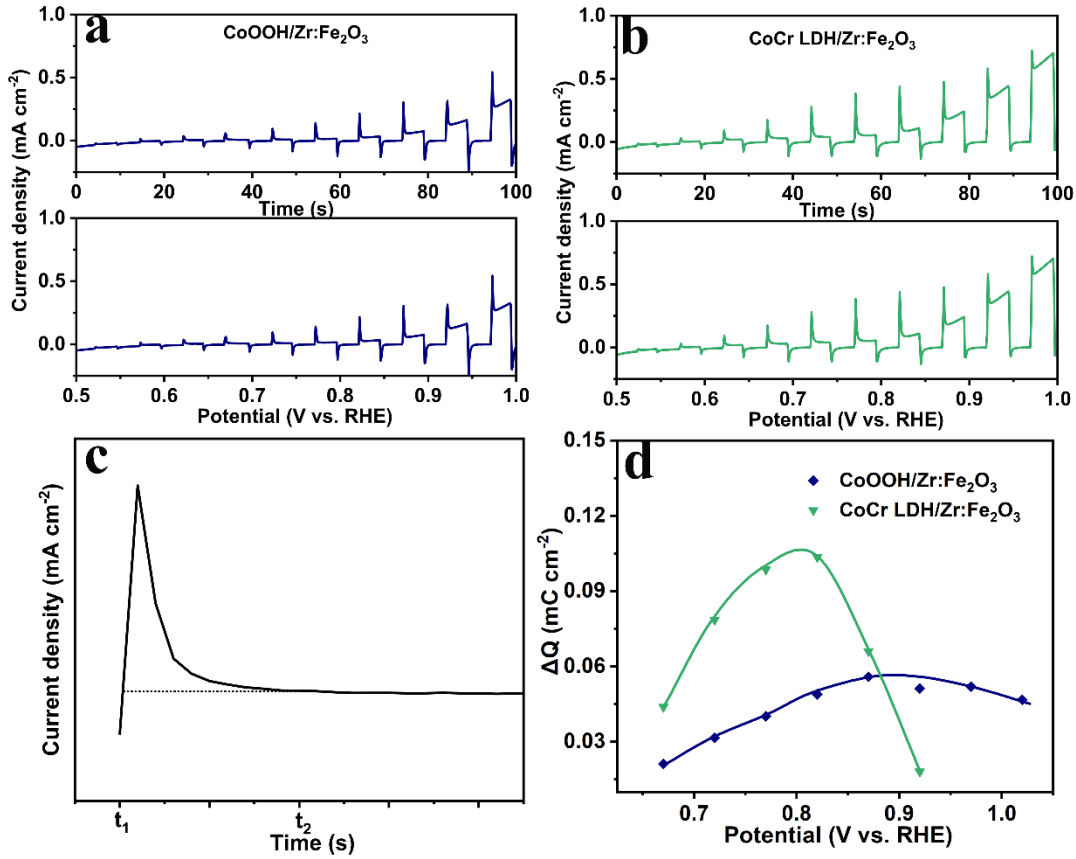

Figure S6. The conversed chronoamperometry curve from LSV curves of (a) CoOOH /Zr:Fe_2O_3 and (b) CoCr LDH/Zr:Fe_2O_3; The potential is scanned from 0.5 to 1.0 V_{RHE} with

5 mV step and a 5 s light on/off cycle on each step. (c) Scheme explaining the data treatment of the anodic current decay; (d) Charge storage of CoOOH/Zr:Fe_2O_3 and CoCr LDH/Zr:Fe_2O_3.

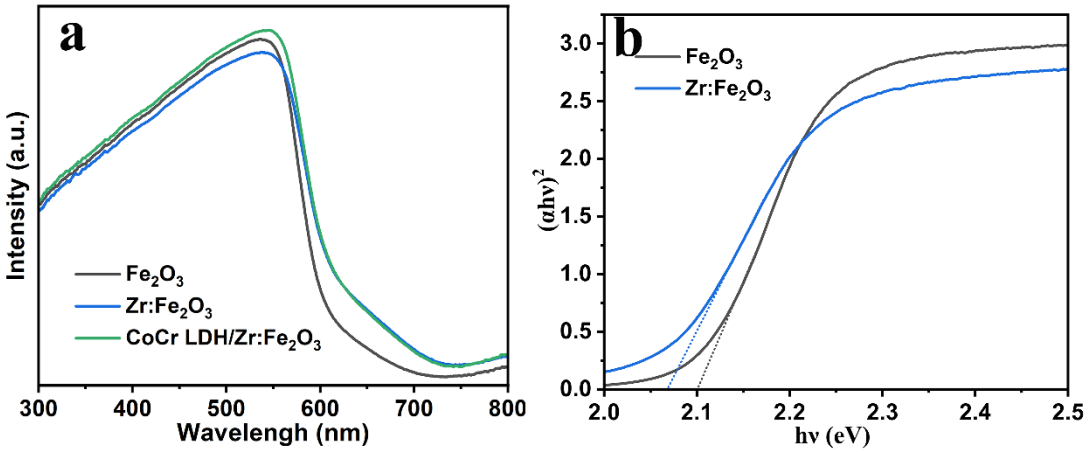

Figure S7. (a) UV-vis spectra of the as-prepared photoanodes and (b) The fitting band gap of hematite based on UV-vis spectrum.

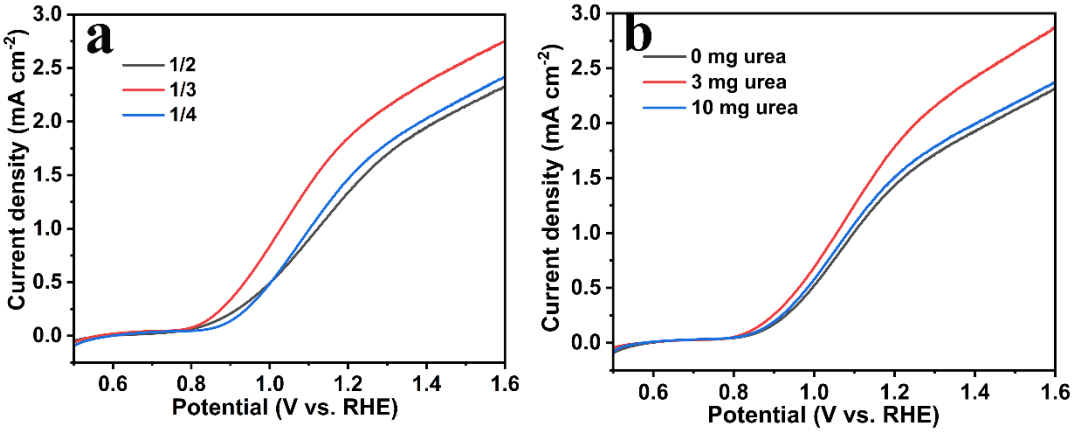

Figure S8. The LSV curves of the composite photoanodes with (a) different molar ratio of Cr^{3+}/Co^{2+} and (b) different contents of urea.

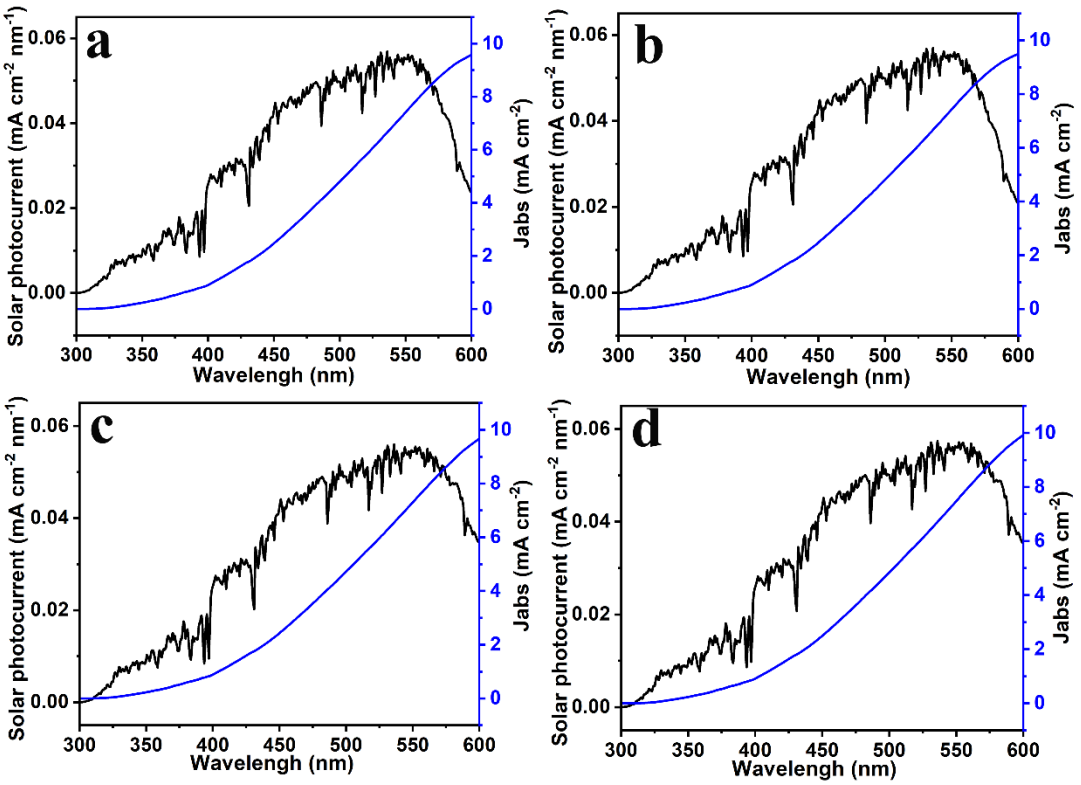

Figure S9. The calculated J_{abs} of (a) Fe_2O_3, (b) CoCr LDH/Fe_2O_3, (c) Zr:Fe_2O_3, and (d) CoCr LDH/Zr:Fe_2O_3 electrodes.

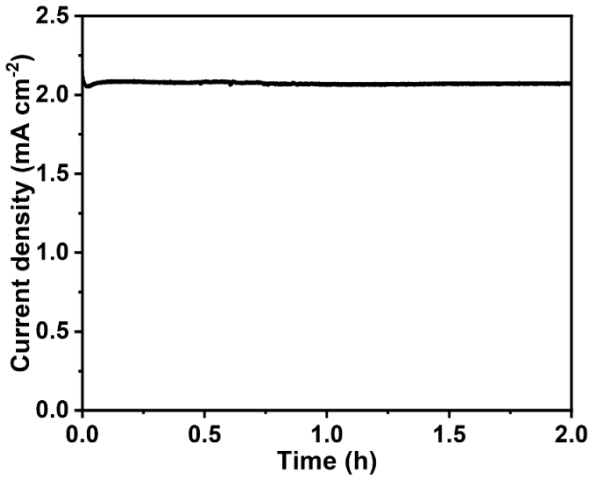

Figure S10. Amperometric i-t curve of CoCr LDH/Zr:Fe_2O_3 electrode measured at 1.23 V_{RHE} under illumination.

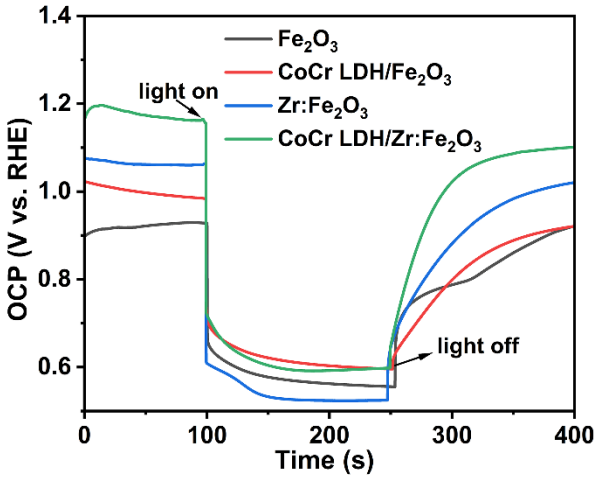

Figure S11. Open circuit potential of all the photoanodes.

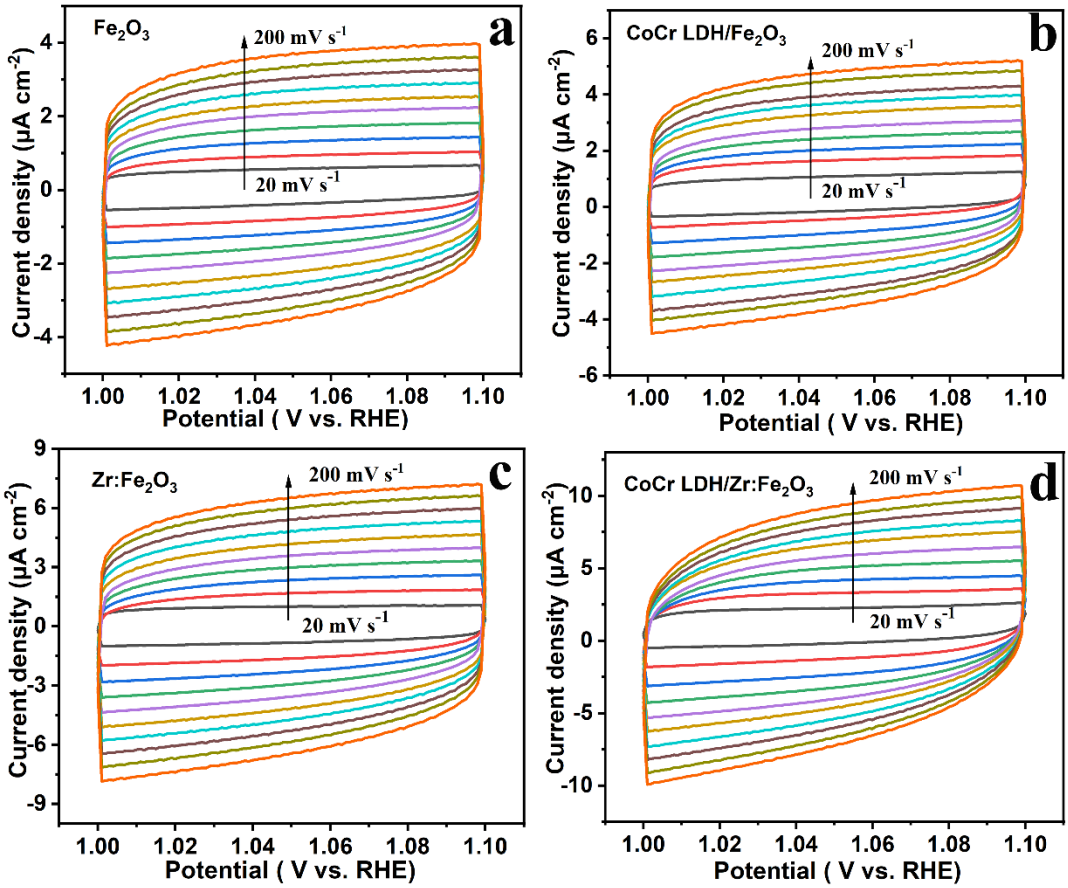

Figure S12. Voltammograms of the (a) Fe_2O_3, (b) CoCr LDH/Fe_2O_3, (c) Zr:Fe_2O_3 and (d) CoCr LDH/Zr:Fe_2O_3 photoanodes at various scan rates (20-200 mV s^{-1}).

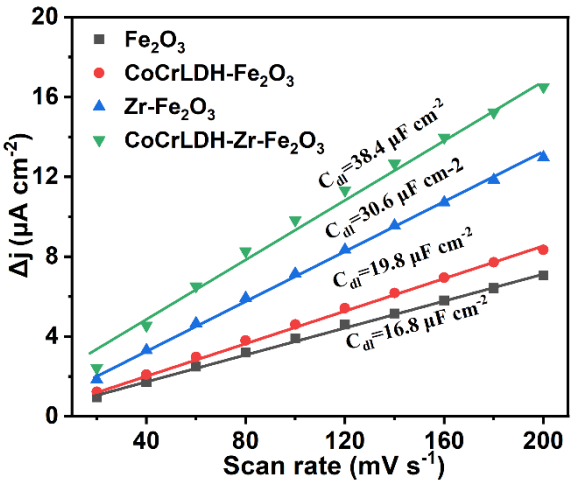

Figure S13. ECSA evaluations of all photoanodes. Charging current differences (Δj=ja–jc) at 1.05 V plotted against scan rate for each photoanode. ja and jc are the anodic and cathodic current in the CV curves of Figure S12, respectively, and the linear slope is twice of the double-layer capacitance (C_{dl}).

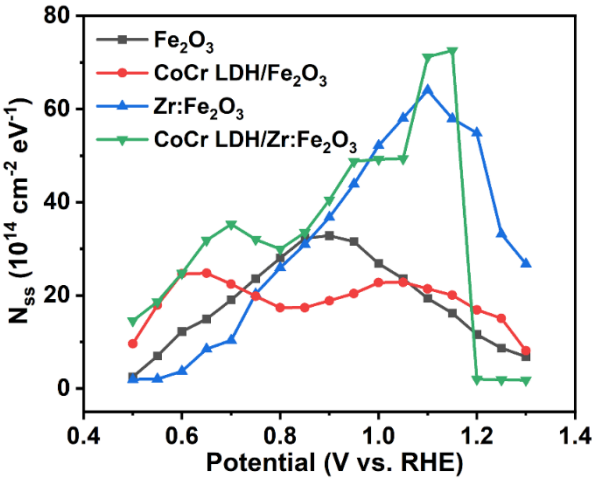

Figure S14. Density of surface states (N_{SS}) of the photoelectrodes as a function of the applied potentials.

The values of density of states (DOS) from C_{SS} were calculated from equation 6:

$$N_{SS}=C_{SS}/e$$

where N_{SS} is the DOS (cm^{-2} eV^{-1}) of the surface states as a function of the potential and e is the electron charge (1.602×10^{-19} C)[4].

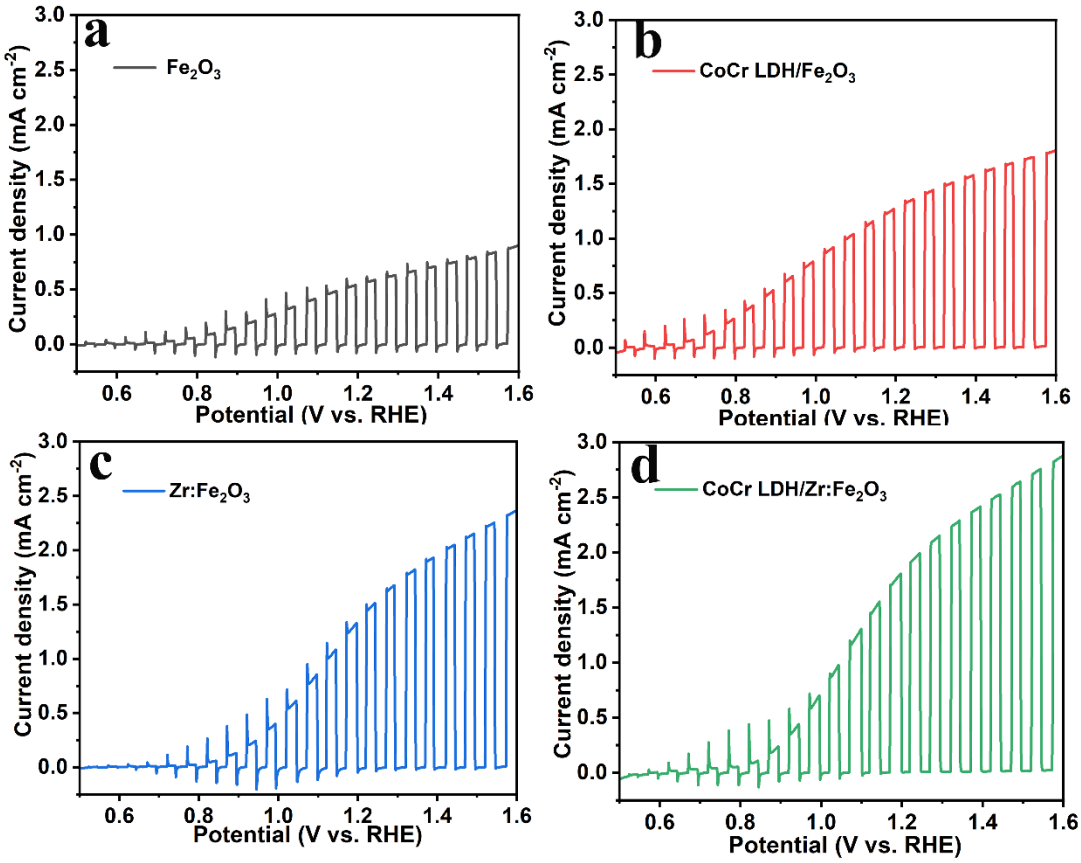

Figure S15. Chopped LSV curves measured in 1 M KOH of (a) α-Fe_2O_3, (b) CoCr LDH/Fe_2O_3, (c) Zr:Fe_2O_3, and (d) CoCr LDH/Zr:Fe_2O_3 photoanodes.

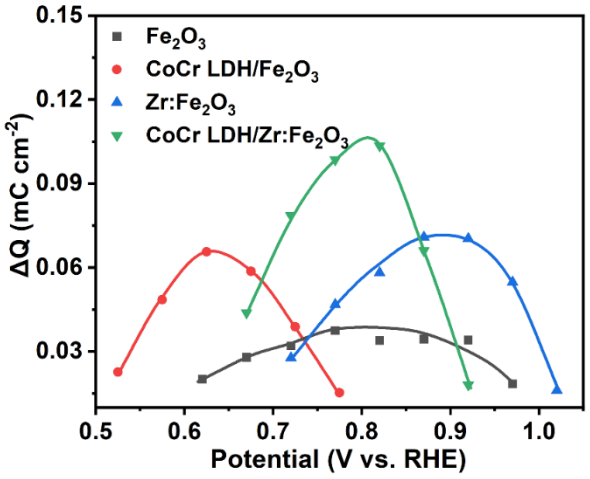

Figure S16. Charge storage of α-Fe_2O_3, Zr:Fe_2O_3, CoCr LDH/Fe_2O_3, and CoCr LDH/Zr:Fe_2O_3 photoanodes.

References

1. T. Hisatomi, J. Kubota and K. Domen, *Chem. Soc. Rev.*, 2014, **43**, 7520-7535.

2. S. Wang, P. Chen, J. H. Yun, Y. Hu and L. Wang, *Angew Chem., Int. Ed.,* 2017, **56**, 8500-8504.

3. F. Li, J. Li, F. Li, L. Gao, X. Long, Y. Hu, C. Wang, S. Wei, J. Jin and J. Ma, *J. Mater. Chem. A*, 2018, **6**, 13412-13418.

4. Q. Shi, S. Murcia-López, P. Tang, C. Flox, J. R. Morante, Z. Bian, H. Wang and T. Andreu, *ACS Catal.*, 2018, **8**, 3331-3342.